Proceedings of the Combustion Institute, Volume 28, 2000/pp. 133–139

# PROBABILITY DENSITY FUNCTION CALCULATIONS OF LOCAL EXTINCTION AND NO PRODUCTION IN PILOTED-JET TURBULENT METHANE/AIR FLAMES

QING TANG,[1] JUN XU[2] AND STEPHEN B. POPE[1]
[1]*Sibley School of Mechanical and Aerospace Engineering*
*Cornell University*
*Ithaca, NY 14853, USA*
[2]*Combustion Design Engineering*
*GE Power Systems*
*Schenectady, NY 12345, USA*

The intense nonlinear interaction between turbulent fluctuations and finite-rate chemistry can cause local extinction and has a strong influence on NO production in non-premixed turbulent flames. Accurate predictions of local extinction and NO formation in turbulent flames require a rigorous means of representing such a strong coupling of turbulence and chemistry and hence are substantial challenges for turbulent combustion models. In this study, a self-contained joint velocity–composition–turbulence-frequency probability density function (PDF) method is used to make calculations of a series of piloted-jet non-premixed flames of methane/air. The ingredients of the present model include the simplified Langevin model for velocity, a stochastic model of turbulence frequency, and the Euclidean minimum spanning tree (EMST) mixing model. An augmented reduced mechanism (ARM2) for methane oxidation, which involves 19 species and 15 reactions (including NO chemistry), is incorporated into the joint probability density function (JPDF) calculations using the *in situ* adaptive tabulation (ISAT) algorithm. The effects of radiative heat loss are studied using an optically thin limit model. The calculation results show good agreement with the experimental data, including the minor species NO and CO. The increase of local extinction with increasing jet velocity is accurately represented by the calculations.

## Introduction

One of the most important issues to address in turbulent combustion calculations is the intense nonlinear interaction between fluid mixing and finite-rate chemistry. Because of the presence of multiple timescales and length scales in turbulent reacting flows, it is computationally prohibitive to perform direct numerical simulations in which the flow, chemistry, and molecular transport processes are described by their fundamental equations. However, in the past decades, several modeling methodologies have been developed to handle realistic finite-rate chemical kinetics with more accurate turbulence models in a practically affordable way. Among these are flamelet models [1], conditional moment closures [2], and probability density function (PDF) methods [3], on the one hand, and reduced chemistry mechanisms [4], intrinsic low-dimensional manifold (ILDM) [5], and *in situ* adaptive tabulation (ISAT) [6], on the other hand.

The work described in the present paper is based on the self-contained velocity–turbulence-frequency–composition PDF method [3,7]. Previous applications of this method to non-premixed turbulent flames have been made by Masri, Subramaniam, and Pope [8], Norris and Pope [7], Saxena and Pope [9], and very recently Xu and Pope [10]. The present work builds on that of Xu and Pope [10], which demonstrates accurate modeling of local extinction and reignition phenomena in piloted-jet non-premixed turbulent flames; these phenomena are considered to be substantial challenges for turbulent combustion models.

Accurate prediction of nitric oxide (NO) formation is another challenge, since the NO reactions are "slow" and $NO_x$ levels in turbulent flames depend on many factors, such as convective residence time, local instantaneous temperature, radiative heat loss, and different NO production mechanisms.

In this paper, the full joint PDF method is used to calculate Barlow and Frank's [11] piloted-jet methane/air flames (namely, flames D, E, and F), including NO formation and radiative heat loss.

## The Flames Considered

The flames D, E, and F represent a series of piloted jet flames measured by Barlow and Frank [11]. The experiment configuration is now briefly summarized, The burner has a fuel nozzle of radius $R_j$

= 3.6 mm and a premixed pilot that extends to a diameter of $D$ = 18.2 mm. The jet fuel is 25% $CH_4$ and 75% air by volume, and the pilot burns a lean premixture of $C_2H_2$, $H_2$, air, $CO_2$, and $N_2$ with the same nominal enthalpy and equilibrium composition as methane/air at an equivalence ratio of 0.77. The bulk velocities of the fuel jet are 49.6, 74.4, and 99.2 m/s for flames D, E, and F, respectively, while the jet Reynolds numbers increase from 22,400 to 44,800.

Strong effects of finite-rate chemistry are observed in these flames, and, starting from flame D, local extinction becomes visible, while flame F has significant local extinction. In each of these flames, the amount of local extinction reaches a peak at an axial distance of about 30 jet radii, with reignition occurring further downstream. Accordingly, the NO levels are strongly influenced by the velocity fields and the burning status of these flames.

## Previous PDF Calculations

PDF methods at different levels have been used to model piloted-jet non-premixed flames of methane. Saxena and Pope [9] modeled a piloted-jet flame using a joint velocity–composition–turbulence-frequency method. The Euclidean minimum spanning tree (EMST) mixing model [12] and a skeletal $C_1$ mechanism consisting of 16 species and 41 reactions were used in the calculations. The skeletal mechanism was implemented using the ISAT algorithm [6]. Their results show that, with the skeletal mechanism, the mass fraction of CO tends to be overpredicted by as much as a factor of 2 on the fuel-rich side.

James et al. [13] calculated flame D using the composition PDF method together with the $k-\varepsilon$ model. They compared the performance of two different simplified chemistry mechanisms: the skeletal mechanism, consisting of 16 species and 41 reactions mentioned above, and a 16-species 12-step augmented reduced mechanism (ARM) [4] without NO chemistry, which we denote by ARM1. Their results proved that the inclusion of $C_2$ species in ARM1 remedies the deficiencies of the skeletal mechanism in the calculation of CO.

Flames D, E, and F have been widely modeled at the International Workshops on Measurement and Computation of Turbulent Non-Premixed Flames [14,15] as main target flames. Several researchers reported PDF calculations of these flames at the Fourth Turbulent Non-Premixed Flames Workshop. The main feature of these computations is that they use the joint composition PDF model, with the mixing model being either IEM [16] or the modified Curl's model [17]. Several different reduced mechanisms and the detailed GRI mechanism with ILDM are used to describe the reactions. Most of these calculations obtained reasonable results for flame D and for flames E and F on the fuel-lean side.

The prediction of NO is also a major concern of the workshop, but the calculation results spread widely compared with the experimental data. In some calculations, the optically thin limit gas radiation model was used to calculate the radiative heat loss and its effects on NO formation, but no clear conclusion on this issue can be drawn from these calculations.

Barlow et al. [18] investigated the effects of radiative heat loss on NO levels in three $H_2/N_2$/air jet flames. The ingredients of their calculations included the joint composition PDF model, a five-step reduced mechanism, and an optically thin limit radiation model. These flames were diluted by helium at different levels, and the jet Reynolds numbers ranged from 8300 to 10,000. They concluded that radiation plays an important role in NO formation in hydrogen jet flames, even though the radiant fractions are relatively low, and an optically thin radiation model is sufficient for the flames studied there.

The velocity–turbulence-frequency–composition joint probability density function (JPDF) method was recently applied to flames D, E, and F by Xu and Pope [10]. Their JPDF method incorporated the EMST mixing model [12] and ARM1 implemented by ISAT. The calculations showed good agreement with the experimental data of mean and conditional mean scalars. And local extinction as well as reignition further downstream were accurately captured by this JPDF-EMST-ISAT-ARM1 approach.

## JPDF Method and Numerical Solution

The joint velocity–composition–turbulence-frequency model contains the following ingredients: The simplified Langevin model [3] is employed for velocity. The turbulence-frequency model used here is that of Van Slooten et al. [19]. The EMST mixing model [12], which models mixing locally in the composition space through interacting particles with neighboring particles, is used.

The modeled JPDF equation is solved by a particle/mesh method implemented in the code *PDF2DV* [20]. This code uses a pseudo-time-marching scheme to solve the stochastic differential equations (SDEs) in many small time steps, $\Delta t$. Statistics of the solution evolve from the specified initial condition until the statistically stationary state of interest is reached. In each time step, separate fractional steps are used to advance the particles in physical, velocity, and composition spaces. The numerical convergence and accuracy of this algorithm were demonstrated by Xu and Pope [21].

The ISAT algorithm is coupled with the *PDF2DV* code to perform the reaction calculations, with the reaction mechanism (denoted by ARM2) being a 19-species (including NO), 15-step augmented reduced

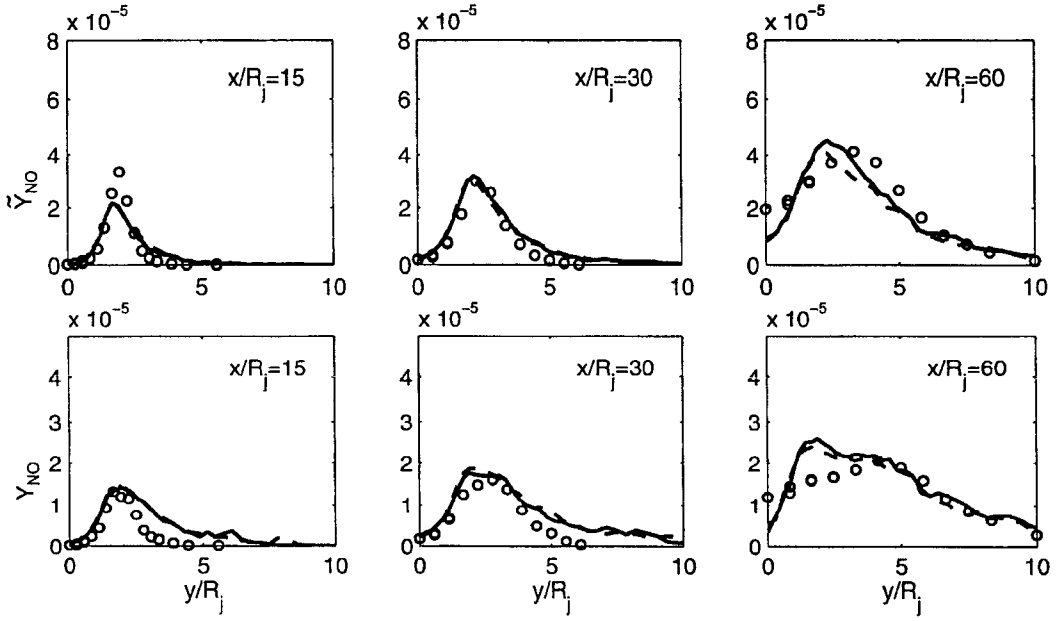


FIG. 1. Radial profiles of unconditional Favre mean and rms NO mass fractions in flame D. Symbols, experimental data; lines, adiabatic calculations.

mechanism derived from GRI-Mech 1.2 for methane oxidation. The ISAT error tolerance, $\varepsilon_{tol}$, is set to be $5.0 \times 10^{-5}$, which can guarantee less then 1% tabulation error for all major species and temperature, less than 10% error for CO and OH , and less than 20% error for NO. An optically thin limit radiation model [22] is implemented in the framework of ISAT. Four gas-phase-emitting species, $H_2O$, $CO_2$, CO, and $CH_4$, are included in this model, and their Planck mean absorption coefficients are calculated by RADCAL [23].

When this paper was at the proof stage (after it was presented at the Combustion Symposium) it was discovered that there was an error in the implementation of radiation in the calculations, and there was insufficient time to repeat the calculations before going to press. The calculations of the radiant fraction and radiative heat loss rate (Fig. 5) are correct. However, the enthalpy of the computational particles remained constant during reaction, rather than decreasing due to radiative heat loss. Hence the calculations previously denoted as "radiant" (the dashed lines in Figs. 1 and 2) are in fact adiabatic; and so the small differences between the solid and dashed lines in Figs. 1 and 2 are due solely to the statistical variability in the calculations. As a consequence, no conclusion can be drawn from these calculations on the effect of radiative heat loss on NO. It should be noted, however, that the results of James and Anand [24] (based on PDF calculations using the same chemistry and radiation models) show that radiation has a negligible effect on NO in these flames (at least up to $x/R_j = 60$).

The calculations are carried out parallelized in a $61 \times 61$ domain with approximately 100 particles per cell. The numerical parameters used are identical to those used by Xu and Pope [10], who thoroughly characterized the numerical accuracy of their computations. From this previous study, it is known that the numerical error in mean and root mean square (rms) profiles are around 10% at $x/R_j \leq 30$, less than 20% at $x/R_j = 60$, but larger at $x/R_j \geq 90$. Statistics conditioned on mixture fraction show considerably less numerical error. While the solution domain used extends to $x/R_j = 120$, results are presented only where the numerical accuracy is assured, namely $x/R_j \leq 60$ for unconditional quantities and $x/R_j \leq 90$ for conditional quantities.

## Results and Discussion

In this section, we present comparisons between the PDF calculations and the experimental data from Barlow and Frank's [11] flames D, E, and F. The PDF calculations have been performed without radiative heat loss.

Figure 1 shows radial profiles of the unconditional Favre mean and rms of NO mass fraction at various axial locations for flame D. It can be seen that the agreement between the calculations and the experimental data is in general very good. The peak value of $\tilde{Y}_{NO}$ at $x/R_j = 15$ is somewhat underpredicted;

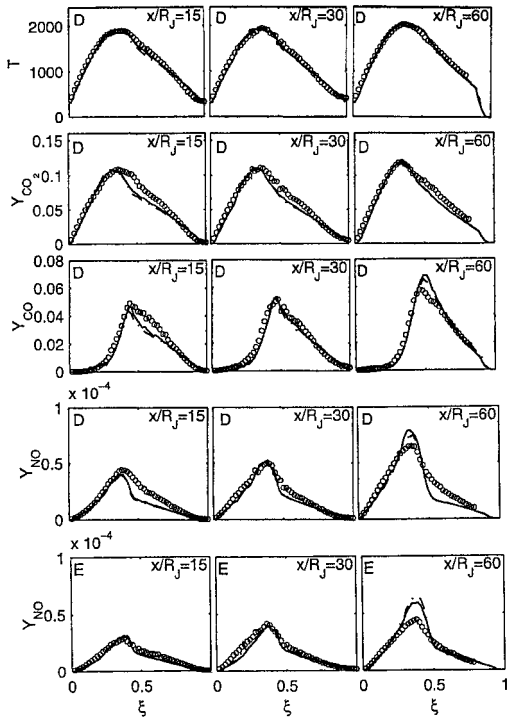


FIG. 2. Conditional means in flames D and E. Symbols, experimental data; lines, adiabatic calculations. (The bottom row of figures is for flame E.)

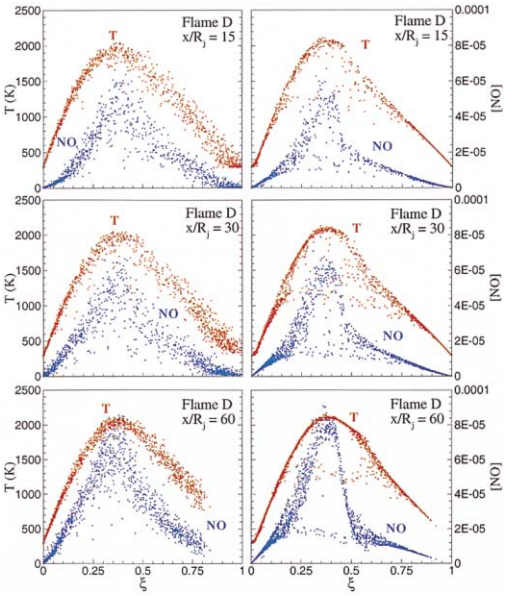


FIG. 3. Scatter plot of temperature and NO mass fractions against mixture fraction ($\xi$) for flame D. Left, experimental data; right, PDF calculations.

but otherwise the calculated levels of $\tilde{Y}_{NO}$ and $Y''_{NO}$ are in excellent agreement with the data.

Figure 2 presents the temperature and $CO_2$, CO, and NO mass fractions conditioned on mixture fraction ($\xi$) at different axial locations for flame D and also the conditional mean of NO for flame E. Although on the fuel-rich side, $CO_2$, CO, and NO are slightly underpredicted at some locations, and at $x/R_j = 60$, the peak values of CO and NO are slightly overpredicted, the calculation results are generally in excellent agreement with the experimental data. Quite similar results are observed in James and Anand's calculations of flame D [24], in which the same ARM2 mechanism was used. In comparison to their results, better predictions were achieved in the present study on the fuel-lean side for CO and NO. For flame E (bottom row in Fig. 2), the lower temperature and shorter residence time compared with flame D leads to lower levels of NO. This effect is accurately represented by the calculations.

Scatter plots of temperature and NO mass fractions versus mixture fraction for flame D are shown in Fig. 3. It is observed that the calculation points are distributed in a narrower band compared with those of the experimental data on the fuel-rich side. Similar results are also observed in Xu and Pope's calculations. This phenomenon is most likely due to deficiencies of the EMST mixing model. Nevertheless, there is in general quite good agreement between the calculations and experiments. The local extinction indicated by sample points with depressed temperature and NO mass fractions in the experiments is accurately captured by the calculations.

A challenge for any turbulent combustion model is to represent accurately the increasing levels of local extinction in flames D, E, and F. Only when the details of turbulence and finite-rate chemistry interaction are described accurately can these local extinction and reignition processes be accurately predicted. A similar challenge is also associated with the prediction of NO formation because the NO chemistry is far from the equilibrium in this situation. A single variable—burning index (BI)—has been introduced by Xu and Pope [10] to quantify the level of local extinction. For a given species, BI is defined as the ratio of the conditional mean mass fraction (conditioned on a mixture fraction range $\xi_l < \xi < \xi_u$) to a reference mass fraction $Y_{|\xi}$, which is chosen so that BI is unity for a mildly strained laminar flame. The burning index for temperature is defined similarly. Generally speaking, smaller BI values indicate more local extinction. Fig. 4 presents the BI of flames D, E, and F at $x/R_j = 30$, where most local extinction occurs. The values of $\xi_l$, $\xi_u$, and $Y_{|\xi}$ are given in the figure caption. The data are extracted from experiments, from Xu and Pope's calculations [10] with ARM1, and from the current study with ARM2.

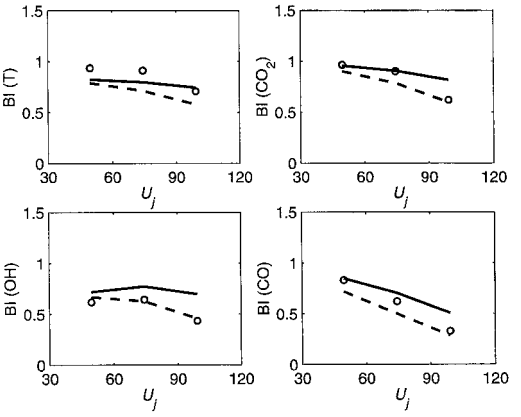


FIG. 4. Burning indices versus jet velocities at $x/R_j$ = 30. Symbols, experimental data; solid line, ARM2 calculations; dashed line, ARM1 calculations (Xu and Pope [10]). For temperature, $\xi_l = 0.30$, $\xi_u = 0.40$, $T_{l\xi} = 2023$ K; for $CO_2$, $\xi_l = 0.30$, $\xi_u = 0.40$, $Y_{l\xi} = 0.1127$; for CO, $\xi_l = 0.43$, $\xi_u = 0.53$, $Y_{l\xi} = 0.05745$; for OH, $\xi_l = 0.28$, $\xi_u = 0.36$, $Y_{l\xi} = 4.527 \times 10^{-3}$.

We first discuss the results for flames D and E and then some special considerations for flame F are described. Especially for $CO_2$ and CO, the results clearly show the increase of local extinction with increasing fuel jet velocity. Both ARM1 and ARM2 show the same trends, with ARM2 being in excellent agreement with the data for $CO_2$ and CO. Since the difference between ARM1 and ARM2 is only in the NO chemistry, it is surprising that such large differences are observed for major species. This may reflect the sensitivity of local extinction to small thermochemical changes in these flames.

For flame F, in Xu and Pope's calculations [10], the pilot temperature is 1860 K, which is suggested by the experimental data and is 20 K lower than that used in the calculations of flames D and E. In this paper, a single pilot temperature (1880 K) is used in all calculations. Thus, for flame F, Fig. 4 does not show a direct comparison between ARM1 and ARM2, because the latter calculation also has a slightly higher pilot temperature. A calculation was also performed with ARM2 and the lower pilot temperature (1860 K), the result of which was that the

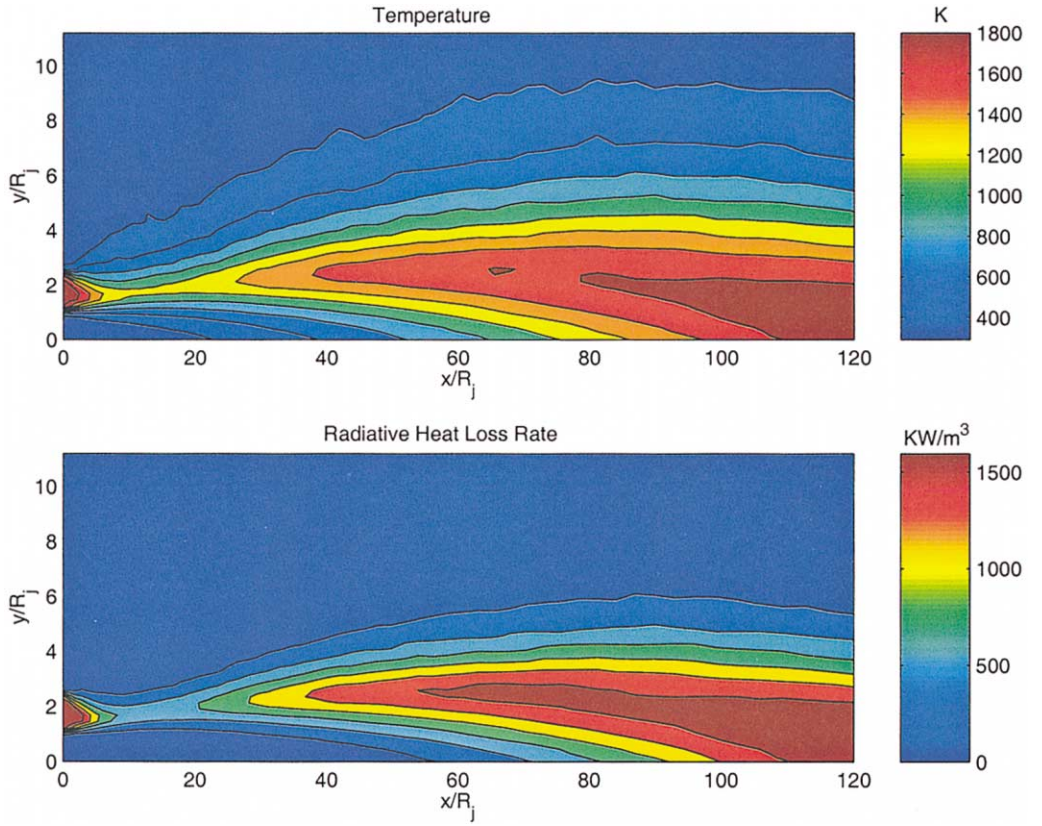


FIG. 5. Contour plots of mean temperature and radiative heat loss rate for flame E.

flame was essentially globally extinguished (at least for $x/R_j \leq 90$). More work is needed to determine whether some of these observations stem from statistical variability in these near-extinction calculations or whether indeed the calculated behavior of the flames is exquisitely sensitive to small changes in the thermochemistry.

Figure 5 presents contour plots of the mean temperature and mean radiative heat loss rate for flame E. The temperature distribution clearly shows the regions where local extinction and reignition processes occur. The calculated total radiant fractions for flames D, E, and F (for $x/R_j \leq 120$) are 2.85%, 1.89%, and 1.12%, respectively, while the measured data (for the entire flame) are 5.1%, 4.1%, and 3.0%, respectively. The tendency for the radiant fraction to drop as the jet velocity increases is well predicted by the calculations, and the smaller calculated values are consistent with the fact that the radiation from $x/R_j > 120$ is not included.

## Conclusions

The results presented here demonstrate that the ARM2 mechanism combined with the JPDF method has the capability to predict accurately NO and CO distributions in non-premixed turbulent flames. The ISAT algorithm makes it possible to incorporate this complicated chemistry in JPDF calculations at a reasonable computational cost, while keeping the errors in the chemistry computations within an acceptable specified tolerance.

The burning index is shown to be a very useful tool to characterize the extent of local extinction. The current calculations can predict the burning index of flames D and E quite accurately. But for flame F, which is very close to extinction, the calculation appears to be very sensitive to the changes of pilot temperature. The experimental data suggest a lower pilot temperature for flame F than for flames D and E. Further investigation is needed to clarify this issue.

The radiant fractions are calculated in this study using an optically thin limit model and are consistent with the measured values.

Improvements in the numerical accuracy and computational efficiency of the algorithm employed are desirable (and are being sought) so that calculations can be made for the downstream portion of the flames, where the effects of radiative heat loss may be more apparent.

### *Acknowledgments*

This work was supported in part by Air Force Scientific Office of Research grant F49620-97-1-0126 and in part by the U.S. Department of Energy, Federal Energy Technology Center, under cooperative agreement no. DE-FC21-92-MC29061 through the Advanced Gas Turbine Systems Research (AGTSR) program. Computations were performed on the Cornell Theory Center's computer. The authors are grateful to Professor A. R. Masri for comments and suggestions on this work.

### REFERENCES

1. Peters, N., *Prog. Energy Combust. Sci.* 10:319–339 (1984).
2. Bilger, R. W., *Phys. Fluids A* 5:436–444 (1993).
3. Pope, S. B., *Prog. Energy Combust. Sci.* 11:119–192 (1985).
4. Sung, C. J., Law, C. K., and Chen, J.-Y., *Proc. Combust. Inst.* 27:295–304 (1998).
5. Mass, U. A., and Pope, S. B., *Combust. Flame* 88:239–264 (1992).
6. Pope, S. B., *Combust. Theory Modelling* 1:41–63 (1997).
7. Norris, A. T., and Pope, S. B., *Combust. Flame* 100:211–220 (1995).
8. Masri, A. R., Subramaniam, S., and Pope, S. B., *Proc. Combust. Inst.* 26:49–57 (1996).
9. Saxena, V., and Pope, S. B., Proc. Combust. Inst. 27:1081–1086 (1998).
10. Xu, J., and Pope, S. B., *Combust. Flame*, in press, (2000).
11. Barlow, R. S., and Frank, J. H., *Proc. Combust. Inst.* 27:1087–1095 (1998).
12. Subramaniam, S., and Pope, S. B., *Combust. Flame* 115:487–514 (1998).
13. James, S., Anand, M. S., Razdan, M. K., and Pope, S. B., in *Proceeding of ASME Turbo Expo Land, Sea & Air 1999*, The Forty-Fourth ASME Gas Turbine and AeroEngine Technical Congress, Indianapolis, IN, 1999.
14. Barlow, R. S., http://www.ca.sandia.gov/tdf/3rdworkshop.
15. Barlow, R. S., http://www.ca.sandia.gov/tdf/4thworkshop.
16. Dopazo, C., *Phys. Fluids A* 18(2):397–410 (1975).
17. Janicka, J., Kolbe, W., and Kollman, W., J. *Non-Equilib. Thermodyn.* 4:47–66 (1979).
18. Barlow, R. S., Smith, N. S. A., Chen, J.-Y., and Bilger, R. W., *Combust. Flame* 117:4–31 (1999).
19. Van Slooten, P. R., Jayesh, and Pope, S. B., *Phys. Fluids* 10:246–265 (1998).
20. Pope, S. B., *PDF2DV, FORTRAN code*, Cornell University, Ithaca, NY, unpublished data, 1994.
21. Xu, J., and Pope, S. B., *J. Comput. Phys.* 152:192–230 (1999).
22. Tang, Q., and Pope, S. B., Report, FDA-99-05, MAE, Cornell University Ithaca, NY.
23. Grosshandler, W. L., RADCAL, NIST Technical Note 1402, U.S. Government Printing Office, Washington, DC, 1993.
24. James, S., and Anand, M. S., Combustion Institute, Central States Section Meeting, Indianapolis, IN, 2000.

# COMMENTS

*R. W. Bilger, University of Sydney, Australia.* I congratulate the authors on their excellent predictions of these important and challenging experiments using our Sydney burner. Our first-order conditional moment closure predictions [1] of flame D overpredicted the extent of the reaction on the rich side of stoichiometric. It seems likely that the Monte Carlo PDF simulations do better because they inherently include the substantial fluctuations in the scalar dissipation rate of the mixture fraction near stoichiometric. For the record, could you please report what these are at several points in the flow? Could you also report what the Reynolds number dependence of these fluctuations is inherent in your mixing model? Is the trend consistent with that reported in the literature?

## REFERENCE

1. Roomina, M. R., and Bilger, R. W., *Combust. Flame,* in press (2000).

*Author's Reply.* It can be observed from the exact PDF equation that molecular mixing affects the PDF through the conditional mean diffusion (independent of conditional fluctuation). In future studies of mixing models, we will extract the conditional mean diffusion; and, with some approximation, the conditional scalar dissipation can then be deduced.

In the modeled PDF equation, mixing occurs at a rate determined by the mean turbulent frequency, and no molecular transport properties are involved. Hence, by construction, the model has no Reynolds number dependence per se. The calculations depend, of course, upon the jet velocity, but it is appropriate to consider this to be a Damköhler-number effect, not a Reynolds-number effect. It would be of great interest for these piloted jet flames to be studied experimentally at different Reynolds numbers but at fixed Damköhler numbers to determine the true Reynolds number dependence.

•

*Jay Gore, Purdue University, USA.* Are the definitions of the radiant fractions in your calculations and in Frank and Barlow's measurements the same? Please note that the wide-angle radiometer measures heat flux leaving all parts of the flame in its view simultaneously. Therefore, the two definitions are likely to be different. Also, can you discuss the origin of differences in the measured and predicted scatter plots?

*Author's Reply.* In experiments, the radiant emission from the entire flame is estimated (although the radiation beyond $x/d = 120$ is neglected). In the calculations, only the radiant emission from the solution domain ($0 \leq x/d \leq 60$) is included. Based on the correlation of Sivathanu and Gore [1], we estimate that the radiant emission in the calculation represents about half of that from the entire flame. The close agreement between measured and calculated scatter plots is very encouraging, especially the correctly predicted trends with jet velocity and downstream distance. It should be appreciated, however, that there are limitations in making quantitative comparisons between the experiments and the calculations. First, the experimental plots contain data from different radial locations. These locations and the number of samples obtained from each are not reported. Second, in the calculations the particles have different numerical weights, but these weights are not distinguished on the scatter plots. Also, only a subset of particles from the calculations is plotted. The differences between the measured and predicted scatter plots are most evident on the fuel-rich side, where the measured sample points are distributed in a wider range than the predicted points. This difference may be due to the stranding tendency of the current EMST mixing model.

## REFERENCE

1. Sivathanu, Y. R., and Gore, J. P., *Combust. Flame* 94:265–270 (1993).